

RESEARCH ARTICLE

HuR inhibition reduces post-ischemic cardiac remodeling by dampening myocyte-dependent inflammatory gene expression and the innate immune response

Samuel Slone^{1,2}  | Sarah R. Anthony^{3,4}  | Lisa C. Green^{1,2}  | Sharon Parkins^{1,3}  |
Pooja Acharya^{3,4}  | Daniel A. Kasprovic^{3,4}  | Kelsi Reynolds⁵  |
Robert M. Jagers^{4,6}  | Michelle L. Nieman²  | Perwez Alam⁷  | Xiaoqing Wu⁸  |
Sudeshna Roy⁹  | Jeffrey Aubé⁹  | Liang Xu⁸  | Zihai Li⁵  | John N. Lorenz²  |
A. Phillip Owens¹  | Onur Kanisicak^{4,6}  | Michael Tranter^{3,4} 

¹Division of Cardiovascular Health and Disease, University of Cincinnati College of Medicine, Cincinnati, Ohio, USA

²Department of Pharmacology and Systems Physiology, University of Cincinnati College of Medicine, Cincinnati, Ohio, USA

³Department of Molecular Medicine and Therapeutics, The Ohio State University Wexner Medical Center, Columbus, Ohio, USA

⁴Dorothy M. Davis Heart and Lung Research Institute, The Ohio State University Wexner Medical Center, Columbus, Ohio, USA

⁵Pelotonia Institute for Immuno-Oncology, The Ohio State University Comprehensive Cancer Center, Columbus, Ohio, USA

⁶Division of Basic and Translational Science, Department of Emergency Medicine, The Ohio State University Wexner Medical Center, Columbus, Ohio, USA

⁷Department of Biomedical Sciences, College of Veterinary Medicine, University of Missouri, Columbia, Missouri, USA

⁸Department of Molecular Biosciences, University of Kansas, Lawrence, Kansas, USA

⁹Division of Chemical Biology and Medicinal Chemistry, Eshelman School of Pharmacy, University of North Carolina, Chapel Hill, North Carolina, USA

Correspondence

Michael Tranter, Department of Molecular Medicine and Therapeutics, The Ohio State University Wexner Medical Center, 2255 Kenny Road, 5181 Pelotonia Research Center, Columbus, OH 43210, USA.

Email: michael.tranter@osumc.edu

Funding information

HHS | NIH | National Heart, Lung, and Blood Institute (NHLBI), Grant/Award Number: HL132111, HL166326, HL148598, F31-HL170636 and HL125204; HHS | NIH | National Cancer Institute (NCI), Grant/Award Number: CA191785, CA243445 and CA252158; American Heart Association (AHA), Grant/Award Number: CDA34110117, PRE35230020, 1029875 and PRE35210795; American Heart Association Postdoctoral

Abstract

The RNA-binding protein human antigen R (HuR) has been shown to reduce cardiac remodeling following both myocardial infarction and cardiac pressure overload, but the full extent of the HuR-dependent mechanisms within cells of the myocardium has yet to be elucidated. Wild-type mice were subjected to 30 min of cardiac ischemia (via LAD occlusion) and treated with a novel small molecule inhibitor of HuR at the time of reperfusion, followed by direct in vivo assessment of cardiac structure and function. Direct assessment of HuR-dependent mechanisms was done in vitro using neonatal rat ventricular myocytes (NRVMs) and bone marrow-derived macrophages (BMDMs). HuR activity is increased within 2 h after ischemia/reperfusion (I/R) and is necessary for early post-I/R inflammatory gene expression in the myocardium. Despite an early reduction in inflammatory gene expression, HuR inhibition has no effect on initial infarct size at 24 h post-I/R. However, pathological remodeling is reduced with preserved cardiac function at 2 weeks post-I/R upon HuR inhibition. RNA sequencing analysis of gene expression in NRVMs treated with

This is an open access article under the terms of the [Creative Commons Attribution-NonCommercial-NoDerivs](https://creativecommons.org/licenses/by-nc-nd/4.0/) License, which permits use and distribution in any medium, provided the original work is properly cited, the use is non-commercial and no modifications or adaptations are made.

© 2025 The Author(s). *The FASEB Journal* published by Wiley Periodicals LLC on behalf of Federation of American Societies for Experimental Biology.

Fellowship, Grant/Award Number:
20POST35200267; American Heart
Association Career Development Grant,
Grant/Award Number: 23CDA1052132

LPS to model damage-associated molecular pattern (DAMP)-mediated activation of toll-like receptors (TLRs) demonstrates a HuR-dependent regulation of pro-inflammatory chemokine and cytokine gene expression in cardiomyocytes. Importantly, we show that conditioned media transfer from NRVMs pre-treated with HuR inhibitor loses the ability to induce inflammatory gene expression and M1-like polarization in bone marrow-derived macrophages (BMDMs) compared to NRVMs treated with LPS alone. Functionally, HuR inhibition reduces macrophage infiltration to the post-ischemic myocardium *in vivo*. Additionally, we show that LPS-treated NRVMs induce the migration of peripheral blood monocytes in a HuR-dependent endocrine manner. These studies demonstrate that HuR is necessary for early pro-inflammatory gene expression in cardiomyocytes following I/R injury that subsequently mediates monocyte recruitment and macrophage activation in the post-ischemic myocardium.

KEYWORDS

cardiac remodeling, heart, HuR, inflammation, innate immune response, ischemia/reperfusion injury

1 | INTRODUCTION

Myocardial ischemia/reperfusion (I/R) injury results in cardiomyocyte cell death and an acute loss of contractile function. The cardiac remodeling that subsequently occurs in compensatory response to I/R is a common underlying cause of heart failure. Specifically, post-ischemic remodeling is known to be driven in part by an increase in the expression of cytokines and chemokines within the ischemic and ischemic border zones of the heart that elicit the innate inflammatory response.^{1–3} Within the first few hours to days, apoptotic and necrotic cell death results in the release of damage associated molecular patterns (DAMPs) that trigger pro-inflammatory signaling through stimulation of toll-like receptors (TLRs) on surviving cells.^{1–3} TLR receptor stimulation then leads to the expression and secretion of critical pro-inflammatory cytokines such as TNF- α , IL-6, and IL-1 β .

The RNA-binding protein Human antigen R (HuR) is a widely expressed RNA-binding protein that is an established mediator of inflammatory cytokine expression.⁴ Indeed, HuR expression has been previously shown to be increased at 3 days post-MI in a mouse model of non-reperfused ischemia.⁵ This same group also showed that HuR inhibition was able to reduce pathological remodeling and preserve cardiac function in this model, in part through abrogation of direct HuR-mediated expression of p53 and TGF- β in macrophages.⁶ However, they did not define the specific role of HuR in cardiomyocytes or the

breadth of HuR-dependent gene expression in myocytes, leaving unanswered questions regarding the functional and mechanistic role of HuR in the acute response to I/R injury.

The primary goals of this work are to show the functional impact of HuR-dependent expression of pro-inflammatory cytokines in cardiomyocytes following I/R and the subsequent effect on post-ischemic cardiac remodeling. To achieve this, we utilized a novel small molecule pharmacological inhibitor of HuR, KH-3, that has been shown to directly compete with HuR-RNA binding in a safe and specific manner *in vivo*.^{7,8} Our results show that HuR inhibition elicits a robust decrease in acute inflammatory gene expression in cardiomyocytes following I/R that, surprisingly, has no effect on the initial infarct or myocyte cell death at 24 h post-I/R. However, in agreement with prior work, HuR inhibition mitigates post-ischemic pathological remodeling and fibrosis, resulting in improved cardiac function at 2 weeks post-I/R. RNA sequencing using neonatal rat ventricular myocytes (NRVMs) treated with a TLR agonist with or without KH-3-mediated HuR inhibition demonstrates an overwhelming majority of HuR-dependent pro-inflammatory genes in response to TLR signaling in cardiomyocytes. Mechanistically, we show that this HuR-dependent inflammatory gene expression in cardiomyocytes mediates the endocrine recruitment and activation of monocytes/macrophages. In sum, this work demonstrates that HuR inhibition provides cardioprotection from post-ischemic remodeling by reducing

pro-inflammatory gene expression in cardiomyocytes and the subsequent activation of the innate immune response.

2 | METHODS

2.1 | Ischemia/reperfusion (I/R) surgery

Ten- to 16-week-old male C57BL/6 mice were obtained from Jackson Labs (stock #000664). I/R surgery was performed as previously described.^{9,10} Briefly, mice were anesthetized under isoflurane, intubated, and ventilated. Following thoracotomy, the left anterior descending (LAD) coronary artery was visualized, and a suture was passed under the LAD distal to the left atrial appendage, immediately after the bifurcation of the major left coronary artery. Ischemia was induced by tightening the suture and confirmed visually by blanching of the ventricle and by electrocardiogram displaying an elevated ST segment. Just prior to loosening the ligation, mice were randomly administered either VEH (5% EtOH, 5% Tween 80, and ddH₂O) or a small molecular inhibitor of HuR denoted as KH-3 (dosed via i.p. injection at 60 mg/kg up to 3× weekly). After 30 min, the suture was released to re-establish blood flow, and the incision was closed in layers. Sham surgeries were performed following the same protocol but without tightening the suture of the left anterior descending coronary artery. All molecular analysis (RNA and protein) was performed using the ischemic zone (and analogous regions from sham treated hearts).

2.2 | Pharmacological inhibition of HuR

HuR was pharmacologically inhibited using the small molecule KH-3, a second generation of HuR inhibitor compounds previously described by Wu et al.¹¹ In vivo HuR inhibition was achieved via i.p. injection of KH3 3× weekly at a dose of 60 mg/kg throughout the study timeline for all 7- and 14-day post-I/R groups, as we have done previously.⁷ For all acute studies (2- and 24-h endpoints), only a single dose of KH-3 was given at reperfusion. In vitro HuR inhibition was achieved using KH-3 at a concentration of 10 μM.

2.3 | Echocardiography

All echocardiographic studies were performed as previously described.^{7,12,13} Briefly, mice were anesthetized under isoflurane and laid in a supine position on a heated platform with ECG recording. Body temperature

was monitored and maintained at 36–38°C. Hair was removed from the chest using a chemical hair remover or an electric razor prior to echocardiography. Using a Vevo 2100, parasternal images were obtained in short and long axes in two-dimensional mode and motion (M)-mode for quantification. These images were then analyzed using VevoStrain software (Vevo 2100, v1.1.1 B1455, Visualsonic, Toronto, Canada) for quantification of cardiac function.

2.4 | Infarct analysis

Mice were anesthetized with isoflurane 24 h after ischemia/reperfusion surgery, and triphenyltetrazolium chloride (TTC) staining was performed as previously described.^{14–16} Briefly, hearts were excised and washed in a heparin/PBS mixture (0.5 mL 1000 U Heparin/10 mL PBS) followed by cannulation of the aorta and perfusion with PBS. The LAD was occluded as for I/R surgery, and hearts were perfused with 150–200 μL of 1% Evans blue. Hearts were then frozen at –20°C for 60 min and then sectioned into six continuous slices 1 mm thick from apex to the occlusion site. Heart sections were incubated in 1% triphenyltetrazolium chloride (TTC) at 37°C for 20 min, followed by a fixation with 10% buffered formalin for 1 h. Images were taken and analyzed using NIH image software (Image J) of the infarct zone (white), risk region (red), and non-risk region (blue).

2.5 | Neonatal rat ventricular myocyte isolation and culture

NRVMs were isolated using collagenase digestion and adhesion differential from fibroblasts as described.^{17,18} Briefly, Sprague Dawley neonatal rats (1–3 days old, Charles River) were decapitated, and the hearts were isolated. Following the removal of the atria, the ventricles were cut into small pieces and digested first in 0.05% trypsin/EDTA (Corning) overnight. The next day, trypsin was aspirated, and hearts were placed in Collagenase II (Gibco) for 15 min in a 37°C water bath followed by 15 min of incubation at 37°C, 5% CO₂. Cells were manually dissociated by trituration, and the supernatant was passed through a 40-μm strainer. Cells were then spun at 100×g, followed by a 40-min pre-plating process on non-treated plates to allow for fibroblast adherence. The non-adherent NRVMs were then transferred to gelatin (0.1%) coated culture-treated dishes in MEM alpha media (Gibco) with 10% FBS and 1% Penicillin–Streptomycin. NRVMs were treated with lipopolysaccharide (LPS) at a concentration of 1 μg/mL, and inhibition of HuR was achieved via siRNA (see below) or via KH3.

2.6 | Bone marrow-derived macrophage (BMDM) isolation and culture

Wild-type C57BL/6 mice were sacrificed using CO₂ and subsequent cervical dislocation followed by removal of the femurs and tibias. BMDMs were then isolated as described^{19,20} with slight modifications. Briefly, once femurs and tibias were cut out and cleaned with ethanol, the end of the bone with visibly less marrow was cut off, and the bones were placed (cut end down) into a 0.5 mL tube with a hole in the bottom, which was then placed in a larger (1.5 mL) tube. Quick pulses for 4–5 s were performed until all or most of the red bone marrow was collected in the outer tube. The collected red bone marrow was distributed into DMEM media (20% FBS and 1% P/S) containing 50 ng/mL of Macrophage colony-stimulating factor (M-CSF) in 100 cm petri dishes and kept in a 37°C, 5% CO₂ incubator. Post 7 days of plating, non-adherent cells were discarded, and BMDMs were re-plated in RPMI media containing 10% FBS and 1% P/S and plated at a density 1.2×10^6 per 1.5 mL for a 6-well plate.

2.7 | Flow cytometry

Cultured BMDMs were lifted with versene and washed three times in PBS before applying F4/80 BUV 395 rat anti-mouse antibody (BD Biosciences, 565614; 1:200 dilution), CD11b PerCP rat anti-mouse/human (eBioscience, 407-0114-80; 1:1000), and CD11c BV711 Armenian hamster anti-mouse (eBioscience, 407-0114-80; 1:1000 dilution) in flow cytometry staining buffer containing DPBS (Gibco, 14190-136) with 0.09% Sodium Azide and 1% BSA. After incubating for 30 min at 4°C, cells were washed and spectral flow cytometry analysis was performed using a Cytex Bioscience Aurora Spectral Analyzer with the following five laser configurations: 355, 405, 488, 561, 640 nm, and 64 detection channels. The spectral signature of unstained, F4/80, CD11b, and CD11c fluorophores was calibrated for spectral unmixing with autofluorescence extraction using single color-stained compensation beads (Invitrogen, 01-3333-42) and unstained cells for autofluorescence. BMDMs were first gated for both F4/80 and CD11b to validate for mature macrophages, and final data is displayed as F4/80^{hi} and CD11c^{hi} cells. Flow cytometry data was generated using FlowJo v.X.X software (BD Biosciences).

2.8 | siRNA-mediated gene silencing

To achieve siRNA-mediated knockdown of HuR expression, NRVMs were seeded at ~75% confluency and

transfected with HuR or non-targeting control siRNA (80 nM) (Santa Cruz Biotechnology) 24 h after plating using Lipofectamine 3000 (ThermoFisher Scientific) as we have previously reported, with ~80% knockdown in NRVMs.¹⁸ Cells were grown for 48 h post-transfection prior to further experimental treatment.

2.9 | RNA isolation and qPCR

RNA was isolated using the Macherey-Nagel NucleoSpin RNA kit. RNA quantity and quality were assessed by optical density at 260 nm and optical density ratios of 260/280 nm and 260/230 nm ratios, respectively. cDNA was synthesized using iScript Reverse Transcription Supermix for RT-qPCR (BioRad). Samples were run on the CFX96 Touch Deep Well Real-Time PCR Detection System (BioRad) using iTAQ Universal SYBR Green qPCR Master Mix (BioRad) to assess levels of 18S, IL-6 (interleukin-6), TNF-alpha (tumor necrosis factor alpha), and IL-1 beta (Interleukin 1 beta). Results were analyzed using the $\Delta\Delta C_t$ method.²¹ Primers are as listed: *18s*: F: 5'-AGTCCCTGCCCTTTGTACACA-3', R: 5'-CCGAGGGCCTCACTAAACC-3'; *IL-6*: F: 5'-CCGAGAGGAGACTTCACAG-3', R: 5'-TGCCATTGCACAACCTCTTTTCTC-3'; *TNF-alpha*: F: 5'-CCCATATACCTGGGAGGAGTCTTC-3', R: 5'-CATTCCTTCACAGAGCAATGAC-3'; *IL-beta*: F: 5'-AACCTGCTGGTGTGTGACGTTTC-3', R: 5'-CAGCACGAGGCTTTTGTGTGT-3'.

2.10 | Protein isolation and Western blotting

Total protein was isolated from in vitro cell cultures and heart tissue using RIPA Buffer with a protease inhibitor cocktail. In addition, nuclear and cytoplasmic fractions were collected from in vivo heart tissue as previously described.²² Briefly, for nuclear/cytoplasmic fractionation, the infarct region was dissected away from the rest of the LV and immediately placed in ice-cold Solution A (10 mM HEPES pH 9, 1.5 mM MgCl₂, 10 mM KCl, 0.5 mM DTT, 0.1% Triton X, and protease inhibitor cocktail), dounce homogenized, incubated on ice for 10 min, and centrifuged at 5000×g for 10 min. The supernatant was saved as the cytoplasmic fraction, while the pellet was resuspended in Solution C (20 mM HEPES pH 7.9, 25% glycerol, 0.6 M KCl, 1.5 mM MgCl₂, 0.2 mM EDTA, 0.5 mM DTT, and protease inhibitor cocktail), incubated on ice for 40 min with vortexing every 10 min, and centrifuged at 10000×g for 15 min. The supernatant was then retained as the nuclear fraction.

For Western blotting, 15 µg of total protein, or a ratio of 10µg nuclear/30µg cytoplasmic extract per lane, was separated on a 10% polyacrylamide gel and transferred to a nitrocellulose membrane. Blocking was performed for 1 h at room temperature using 5% bovine serum albumin in a 0.1% Tween 20 Tris-buffered saline (T-TBS) solution. Primary antibodies for HuR (Abcam, ab200342; 1:2000), Periostin (Novus, NBP1-30042; 1:1000), Histone H3 (Cell Signaling, 4499S; 1:1000), CD68 (BioRad, MCA1957; 1:500), and GAPDH (Cell Signaling, 2118S; 1:2000) were incubated overnight at 4°C in 5% BSA, and secondary antibodies (1:5000) were incubated for 1 h at room temperature in 5% BSA. Protein loading was normalized using Stain Free total protein per manufacturer's instructions, Histone H3 (nuclear) or GAPDH (cytoplasmic), as appropriate.

2.11 | Histological analysis

Mouse hearts were isolated and embedded in Tissue-Tek OCT compound, then rapidly frozen in an acetone and dry ice slurry. Frozen hearts were sectioned at 7µm thickness and were subsequently post-fixed and processed for histological analysis. Sections were stained with Picrosirius Solution B (Polysciences, 24901B) for one hour, washed in 0.1 M HCl, and then dehydrated and cleared through ethanol and xylene washes, according to the manufacturer's protocol. Immunostaining of macrophages was performed using a CD68 antibody as previously described.²³ Briefly, sections were incubated in blocking solution (5% BSA, Sigma Aldrich) for 30 min, followed by primary CD68 antibody for one hour and AlexaFluor secondary antibody (Thermo Fisher Scientific A11008) for 30 min. TUNEL staining was performed using a commercial kit (In Situ Cell Death Detection Kit, TMR (Sigma, 12156792910)) according to the manufacturer's protocol. Briefly, frozen sections were post-fixed with paraformaldehyde, followed by permeabilization (0.1% triton X-100), then incubated with TUNEL reaction mixture at 37°C, and nuclei were counterstained with DAPI. All images were captured on a BioTek Cytation 5 imager and analyzed in Image J.

2.12 | RNA sequencing and gene ontology analysis

RNA was isolated from NRVMs as described above, and 300ng total RNA was sequenced using 100 base pair paired-end reads at a total depth of approximately 40 million reads per sample. Genomic mapping of sequence reads and differential expression analysis, using a statistical threshold of a false discovery rate (FDR)-corrected p -value $\leq .01$ and fold-change ≥ 2 , principal component analysis (PCA), heat mapping, and Venn diagram creation was done using the

Qiagen CLC Genomics Workbench (version 21.0.3) as previously described.^{7,13,24} All RNA-Seq raw data files and total gene count files have been deposited to the NCBI GenBank (GSE Accession Number 235081).

Subsequently, gene ontology (GO) analysis of differentially expressed genes was done using the NIH DAVID Bioinformatics Functional Annotation Tool (<https://david.ncifcrf.gov>) with a statistical threshold of FDR p -value $\leq .01$ and ≥ 5 total genes per GO term.^{25,26} GO enrichment and volcano plots were created using RStudio (version 2023.06.1+524) on macOS.

2.13 | PBMC isolation and migration assay

Peripheral blood mononuclear cells (PBMCs) were isolated from the blood of adult rats as previously described.²⁷ Briefly, PBMCs were obtained using the Ficoll-Paque centrifugation (GE Healthcare, 17-5446-02), according to the manufacturer's instructions. Following isolation, PBMCs were plated into the inserts of the migration chamber at a concentration of 1×10^6 per well. The protocol for the migration assay is described by the manufacturer's protocol (CellBioLabs).

2.14 | Statistical analysis

Statistical analysis was performed using GraphPad PRISM 9 software. All graphed results are presented as the mean \pm standard deviation. Results were analyzed with unpaired Student's t -tests, one-way ANOVA, or two-way ANOVA as appropriate, and statistical significance between groups was considered at $p \leq .05$.

2.15 | Study approval

All animal procedures were performed with the approval of the Institutional Animal Care and Use Committee at the University of Cincinnati and the Ohio State University in accordance with the NIH Guide for the Care and Use of Laboratory Animals.

3 | RESULTS

3.1 | Cytoplasmic and total HuR protein are increased following I/R

Krishnamurthy et al. previously showed that total HuR expression is increased at 3 days post-I/R, and

shRNA-mediated knockdown of HuR reduced inflammatory signaling at 3 days post-MI.^{5,6} To determine if HuR is acutely activated in the infarcted myocardium, wild-type C57BI/6 mice were randomized to either 30 min of LAD occlusion or sham surgery, followed by 2 h of reperfusion. Western blot analysis shows a significant increase in HuR nuclear-to-cytoplasmic translocation in the ischemic zone of I/R hearts compared to sham at 2 h post-reperfusion (Figure 1A,B). In addition, total protein collected from the LV ischemic zone shows that increased total HuR expression in I/R hearts compared to sham mice persists at seven days post-I/R (Figure 1C,D). These results show that HuR is activated as soon as 2 h post-I/R, and the total expression level remains increased for at least 7 days.

3.2 | HuR inhibition blunts early pro-inflammatory cardiac cytokine expression, but does not impact acute infarct size

To determine the functional impact of HuR signaling in the acute response to I/R injury, mice were treated with a small molecule inhibitor of HuR (KH-3; HuRi) or vehicle control at the time of reperfusion. Results show that HuR inhibition (HuRi) blunts the I/R-mediated increase in IL-6 and TNF- α gene expression in the infarct zone at 2 h post-reperfusion (Figure 1E,F). However, HuR inhibition had no effect on the initial infarct at 24 h post-I/R as determined by TTC staining (Figure S1). In addition, TUNEL staining performed on cardiac sections spanning the infarcted regions of the heart showed no significant

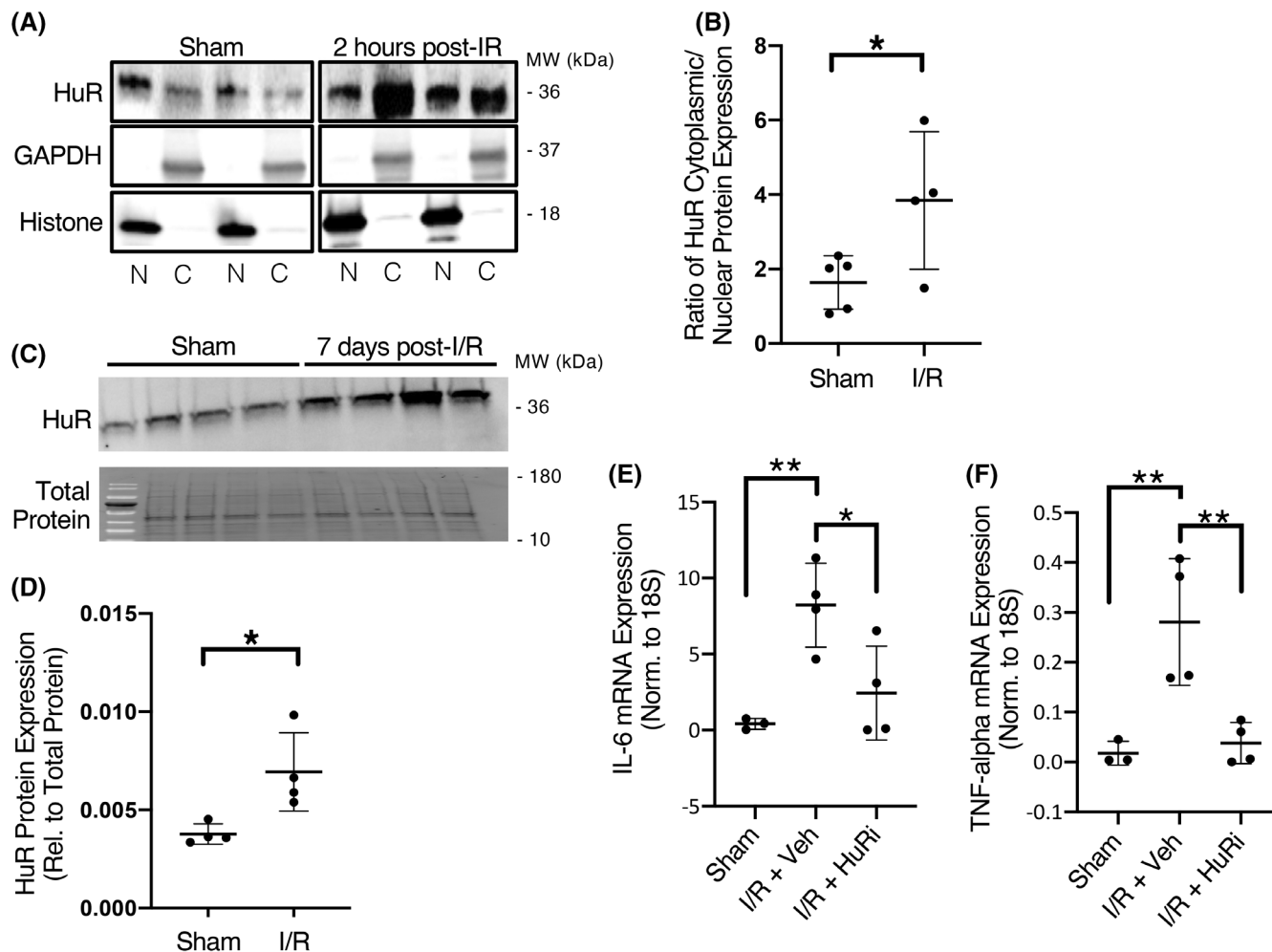


FIGURE 1 HuR activation and expression is increased following I/R injury. HuR cytoplasmic translocation, indicative of activation, is increased at 2 h post-I/R (N and C represent nuclear and cytosolic fractions, respectively) (A). Cytoplasmic translocation of HuR is quantified in panel B. Total HuR protein expression is increased in hearts at 7 days post-I/R (C, D). Treatment with the HuR inhibitor KH-3 (50 mg/kg) at the time of reperfusion reduces expression of pro-inflammatory gene expression of IL-6 (E) and TNF- α (F) at 2 h post-reperfusion. * $p \leq .05$. ** $p \leq .01$.

differences in the percentage of TUNEL-positive cells between mice treated with vehicle and HuRi (Figure S2).

3.3 | HuR inhibition decreases post-ischemic ventricular remodeling and cardiac fibrosis

Cardiac structure and function were assessed via echocardiography at 2 weeks post-I/R to determine the functional effect of HuR inhibition. HuR inhibition blunts the post-ischemic increase in left ventricular (LV) end-diastolic and LV end-systolic volume at 2 weeks following I/R (Figure 2A,B), while preserving cardiac ejection fraction (Figure 2C) compared to vehicle-treated mice. Additionally, mice that received HuR inhibitor displayed less total fibrosis at 2 weeks post-I/R as assessed by picrosirius red staining (Figure 2D,E). Consistent with a reduction in total fibrosis, protein expression of periostin, an indicator of activated myofibroblasts, was also significantly decreased at 2 weeks post-I/R upon HuR inhibition (Figure 2F,G).

3.4 | HuR mediates the expression of inflammation and immune response-related genes in myocytes following LPS stimulation

To begin to delineate the mechanisms of HuR-dependent effects within cardiomyocytes in the post-ischemic myocardium, we utilized a model of cultured neonatal rat ventricular myocytes (NRVMs) treated with LPS to elicit toll-like receptor (TLR) receptor signaling, similar to what would be observed downstream of damage-associated molecular patterns (DAMPs) that often occur during in vivo I/R injury.¹⁻³ In accordance with our in vivo results, we observed increased nuclear-to-cytoplasmic translocation of HuR at 1 h following LPS treatment (Figure S3), and RNA sequencing to identify the HuR-dependent transcriptomic changes was performed at 2 h post-treatment to mirror the in vivo timepoint at which we show increased HuR activity and HuR-dependent IL-6 and TNF- α expression (Figure 1).

Principal component analysis (PCA; Figure 3A) and gene expression heat map (Figure 3B) were used to visualize broad-level changes in the transcriptome and demonstrate clear changes in the transcriptome from NRVMs treated with LPS, LPS plus HuR inhibitor, or vehicle control for 2 h. We next applied differential expression analysis using a statistical cutoff of an FDR-adjusted p -value ≤ 0.01 and fold-change ≥ 2 and found 1911 total differentially expressed genes following LPS treatment (compared to vehicle), with 1113 of these LPS-dependent expression changes also dependent on HuR (Figure 3C,D; Table S1). Volcano

plot representation of these LPS-dependent gene expression changes shows the majority of LPS-dependent expression changes to be increased (Figure 3C), whereas HuR inhibition reversed many of these LPS-dependent changes (Figure 3D). Gene labels in Figure 3C,D represent significant differentially expressed genes from the *Immune System Process* gene ontology grouping (GO:0002376) that were found to be the most significant HuR-dependent GO group of regulated genes following LPS in NRVMs (Figure 3H), and these genes exemplify the LPS-dependent increase in expression that is reversed with HuR inhibition.

Gene ontology (GO) enrichment analysis was used to provide functional insight into these changes in gene expression and showed a significant enrichment in inflammation and innate immune response-related GO terms following LPS treatment (Figure 3E,F). Unsurprisingly, the top 10 enriched LPS-dependent GO terms among up-regulated genes in myocytes, as ranked by p -value, are all related to inflammation or the innate immune response (Figure S4). Conversely, only 11 GO terms were significantly enriched among the LPS downregulated genes, and these were predominately associated with the DNA damage response and DNA repair (Figures 3F and S5).

Importantly, of the 72 significantly enriched HuR-dependent GO terms derived from genes whose expression was significantly increased following LPS stimulation, 56 (78%) of these were related to inflammation or the innate immune response, indicating these pathways to be primarily HuR-dependent downstream of TLR signaling in myocytes (Figure 3G,H). On the other hand, among genes significantly downregulated following LPS stimulation, very few (only three) of these significantly downregulated GO enrichments were found to be HuR-dependent (Figure S6).

These results, showing that HuR primarily mediates increased gene expression following LPS treatment, are not surprising given the primary role of HuR in stabilizing and thus promoting increased expression of mRNA targets. It is also worth noting that the majority of the significant LPS-dependent gene expression changes (1040/1911; 54%) were LPS-induced increases in expression, and 617 of these (59%) were found to also be HuR-dependent (Table S1). Taken together, these results suggest that HuR plays a significant role in the LPS/TLR-dependent increases in inflammatory and innate immune system-related gene expression in myocytes.

3.5 | Cardiomyocytes induce inflammatory gene expression in macrophages via a HuR-dependent endocrine mechanism

As HuR-dependent gene expression in myocytes appears to be independent of myocyte cell death or acute infarct size,

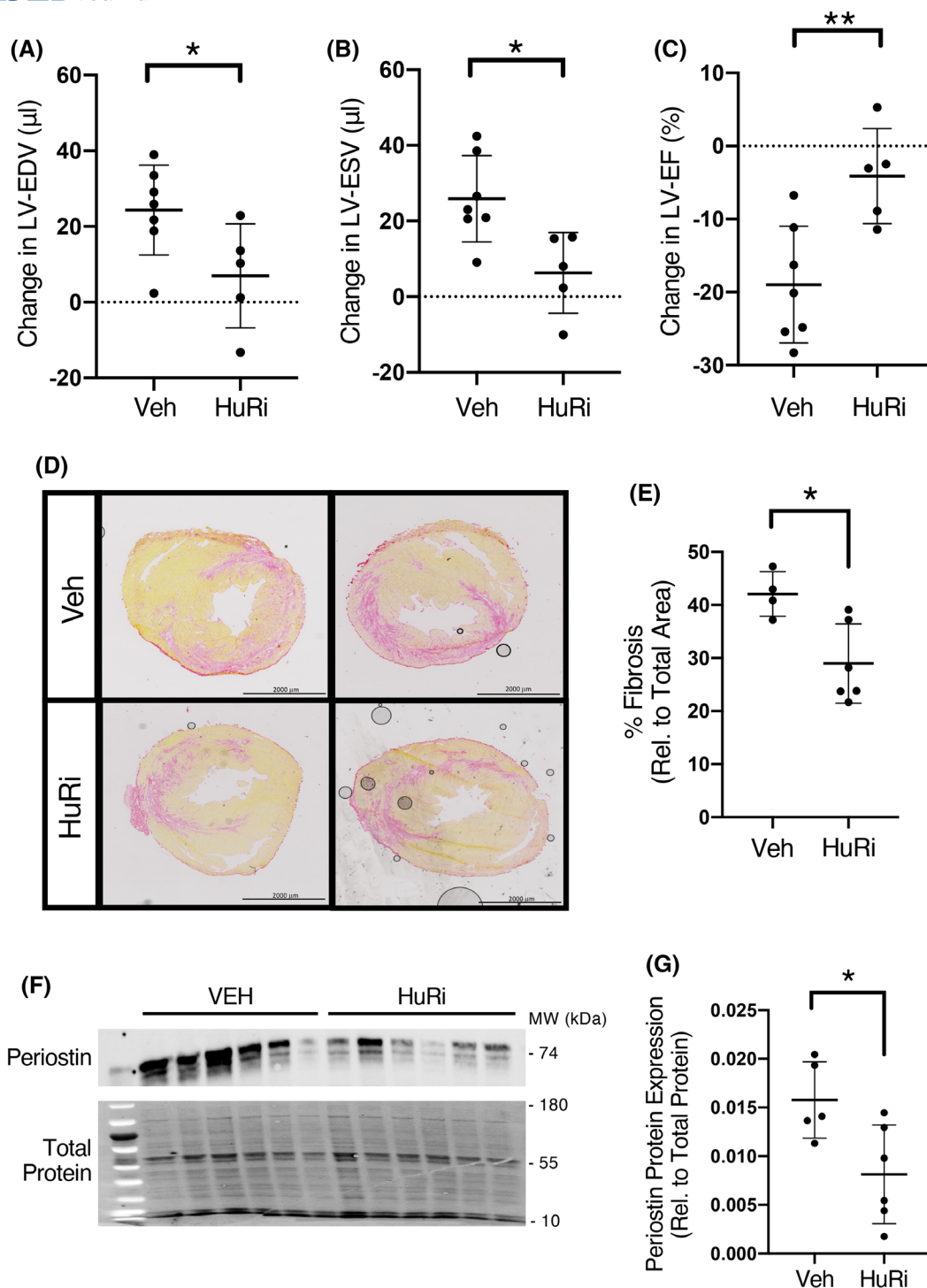


FIGURE 2 HuR inhibition reduces post-ischemic cardiac remodeling and preserves cardiac function. HuR inhibition significantly reduced post-ischemic cardiac remodeling as assessed by LV end-diastolic volume (A) and end-systolic volume (B) and preserved LV function (ejection fraction; C) at 2 weeks post-I/R. Treatment with HuRi also reduced total cardiac fibrosis as determined by picrosirius red staining (D; quantified in E) and myofibroblast activity as assessed by total expression of the myofibroblast marker periostin (F; quantified in G). * $p \leq .05$. ** $p \leq .01$.

we next sought to determine if these HuR-dependent gene expression changes in myocytes might have an impact on post-ischemic remodeling through endocrine effects to other cell types. Recruitment and activation of the innate

immune response are known to play a substantial role in post-ischemic cardiac remodeling.¹⁻³ Indeed, we observe a decrease in macrophage infiltration to the myocardium at 7 days post-I/R upon HuR inhibition (Figure 4A,B).

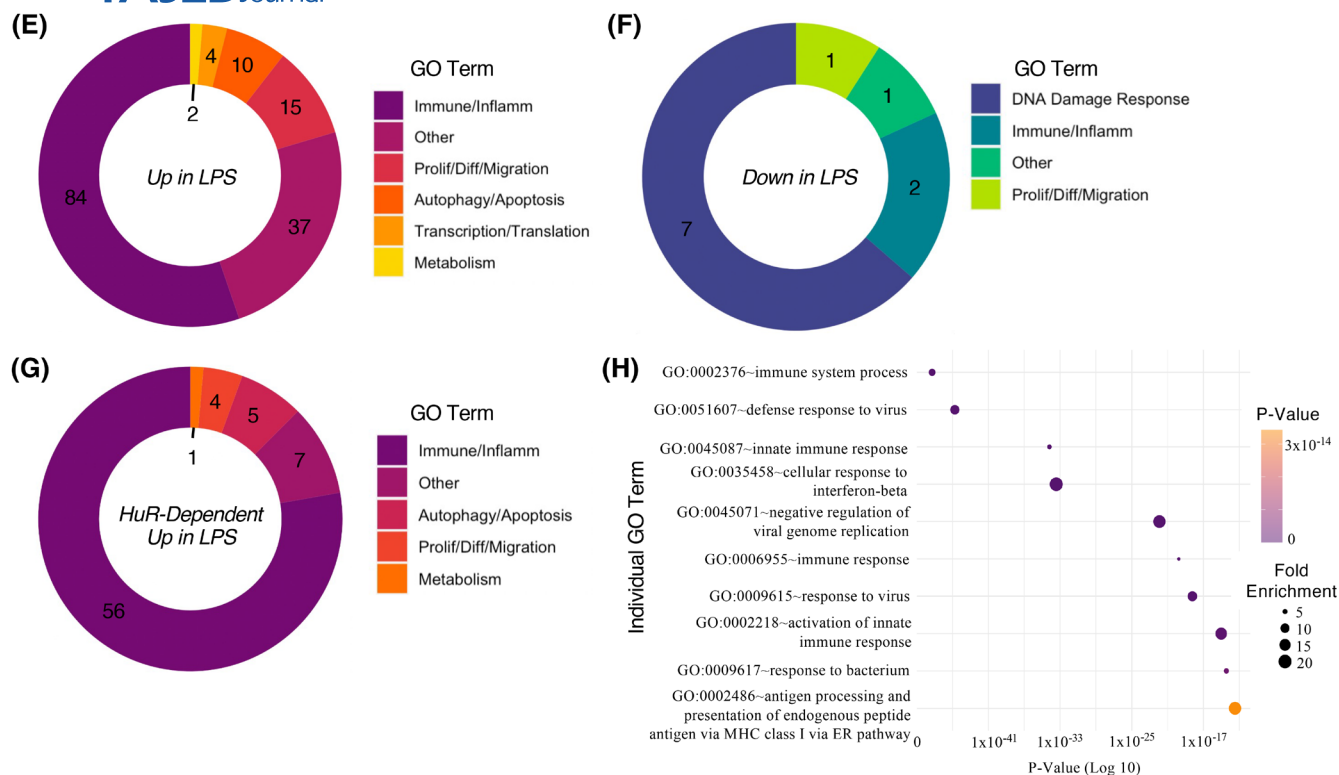


FIGURE 3 (Continued)

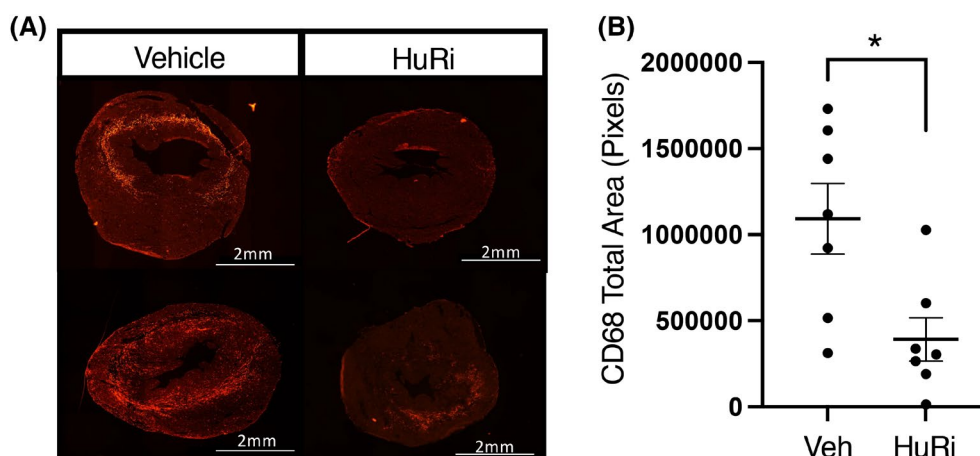


FIGURE 4 HuR inhibition reduces macrophage infiltration to the post-ischemic myocardium. Immunofluorescent staining of CD68⁺ cells shows a reduction in macrophage infiltration to the heart at 7 days post-I/R upon HuR inhibition (A; total area of CD68⁺ stain is quantified in B). * $p \leq .05$.

conditioned media from LPS-treated NRVMs increase the percentage of F4/80^{hi}, CD11c^{hi} recipient BMDMs, suggestive of an M1-like BMDM polarization (Figure 5H,I). However, concomitant with our other results demonstrating reduced inflammatory signaling when HuR activity is blunted via KH-3 or siRNA, conditioned media from NRVMs treated with the commercially available HuR inhibitor DHTS reduce M1-like BMDM polarization (Figure 5H,I).

Importantly, we next utilized a peripheral blood mononuclear cell (PBMC) migration assay to determine whether the HuR-dependent endocrine signaling from myocytes is sufficient to induce functional changes in the migratory nature of these cells to the myocardium following ischemic injury. NRVMs were again treated with LPS alone or LPS plus HuR inhibitor, and conditioned media was transferred to the top half of a migration chamber containing isolated PBMCs. Results demonstrate increased PBMC

migration when exposed to conditioned media from NRVMs treated with LPS alone, but this migratory effect is lost upon HuR inhibition in the NRVMs (Figure 5J).

4 | DISCUSSION

The results presented herein demonstrate that pharmacological inhibition of HuR reduces pathological remodeling and preserves cardiac function in a mouse model of I/R injury. Furthermore, the initial dose of HuR inhibitor in this study was given at the onset of cardiac reperfusion (following a 30-min ischemia) reflecting a clinically relevant timepoint that may be achievable in a human study should an approved inhibitor of HuR become available. To this end, HuR has been well-studied as an oncogene in multiple human cancers, and the clinical development of HuR inhibitors is being actively sought as cancer therapeutics.^{8,28–32} However, not as much is known regarding the functional role of HuR in cardiovascular diseases, but our lab and others have shown that HuR expression is increased in failing human hearts.^{7,33} Our previous work applied the same pharmacological inhibitor used in this study to show that HuR inhibition reduces pathological cardiac remodeling in a mouse model of chronic pressure overload.⁷ Chronic cardiac pressure overload (e.g., hypertension or aortic stenosis) and ischemic injury are two of the most common underlying causes of heart failure, but the molecular mechanisms by which each progresses are distinctly different at the cellular level.

Previous work showed that the administration of the anti-inflammatory cytokine IL-10 mitigates cardiac remodeling and dysfunction following chronic cardiac ischemia in a permanent ligation myocardial infarction (MI) model, in part through the suppression of HuR expression.⁵ This same group subsequently showed that direct knockdown of HuR via shRNA yielded a similar reduction in remodeling and preserved function.⁶ However, while they did show elevation of total HuR protein levels as early as 3 days post-MI,⁵ the acute effects of HuR-dependent signaling in the early response to ischemia (or reperfusion) were not addressed. Our results here show that total HuR expression is elevated at 7 days post-I/R, but we also demonstrate that nuclear-to-cytoplasmic translocation of HuR, indicative of HuR activation, is increased as early as just 2 h after reperfusion. This is an important consideration not only for how the initial ischemic infarct size may affect subsequent remodeling (e.g., a smaller initial cardiac infarct size may mask a differential chronic remodeling effect) but also for the mechanistic understanding of how HuR mediates the observed changes in cardiac structure and function.

We initially hypothesized that HuR inhibition would suppress inflammatory gene expression in the acute phase (0–24 h post-I/R) and result in a subsequently smaller initial cardiac infarct size at 24 h post-I/R. Thus, while our results showing reduced pathological remodeling and preserved function at 2 weeks post-I/R corroborate previously published work, our results showing no effect of HuR inhibition on acute infarct size were surprising. Despite this, HuR inhibition did blunt early (2-h post-I/R) inflammatory gene expression *in vivo*, a result that we were able to replicate using a direct LPS-mediated stimulation of TLRs in NRVMs *in vitro*. Application of RNA sequencing in NRVMs treated with LPS with and without HuR inhibition also showed that the overwhelming majority of HuR-dependent genes in these cells following LPS stimulation associate with inflammation-related gene ontology categories.

Interestingly, the unique transcriptome profiles represented by the PCA plot in Figure 3A demonstrate that many of the LPS-induced changes in gene expression are not HuR-dependent. Thus, while blunting the HuR-dependent aspect of LPS-mediated gene expression changes in NRVMs is sufficient to reduce their subsequent activation of macrophages, HuR inhibition does not simply revert the LPS-induced gene expression back to a basal state. Indeed, many of the HuR-dependent inflammatory gene products are secreted cytokines and chemokines that would exert likely paracrine or endocrine effects on other cells. However, as HuR acts at the post-transcriptional level and is not expected to interfere with LPS-mediated transcriptional changes, the presence of many HuR-independent changes downstream of LPS is not surprising, but it remains to be seen which LPS-dependent functions remain intact in KH-3 treated cells.

Our results also show that HuR inhibition significantly reduces the number of CD68⁺ macrophages in the myocardium at 7 days post-I/R. HuR has been previously shown to control the expression of inflammatory cytokines in multiple cell types, including macrophages.^{4,34–39} Thus, our *in vitro* data using conditioned media from NRVMs treated with HuRi is important to demonstrate a HuR-dependent, cardiomyocyte-driven endocrine recruitment and/or activation of monocytes/macrophages as a likely mechanism. Deeper mechanistic studies, including inhibition of specific cytokine signaling within the recipient macrophages, will be needed to conclusively identify the responsible secreted factor, but our results clearly show that HuR-dependent secreted factors from NRVMs following TLR stimulation are sufficient to induce inflammatory signaling in macrophages. Importantly, not only are these HuR-dependent secreted factors capable of activating naïve M0-like macrophages *in vitro*, which may be most relevant to the existing pool

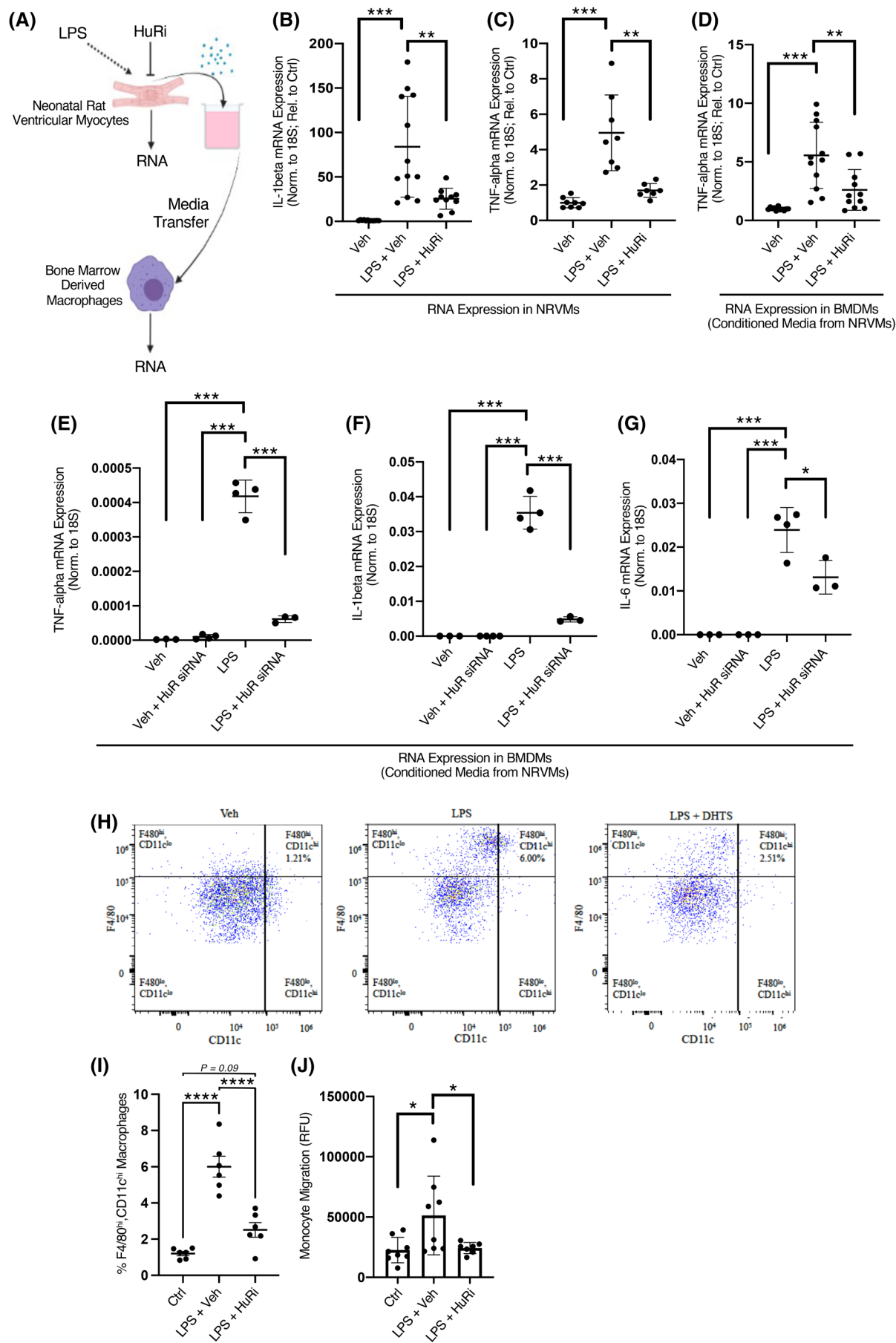


FIGURE 5 TLR signaling in myocytes induces inflammatory gene expression in macrophages in a HuR-dependent endocrine manner. Schematic representation of NRVm treatment and conditioned media transfer to BMDMs (A). HuR inhibition reduces mRNA expression of IL-1 β (B) and TNF- α (C) directly in NRVms. Conditioned media from LPS-treated NRVms induces expression of TNF- α in BMDMs that is blunted when NRVms are treated with HuR inhibitor (D). siRNA-mediated knockdown of HuR in NRVms inhibits the LPS-mediated increase in TNF- α (E), IL-1 β (F), and IL-6 (G) in BMDMs treated with conditioned media from NRVms. Flow cytometric analysis of BMDMs shows an increase in the percentage of F4/80^{hi}, CD11c^{hi} BMDMs following treatment with conditioned media from LPS treated NRVms that is blunted when NRVms are treated with a HuR inhibitor (H, I). Conditioned media transfer from NRVms treated with LPS induces monocyte (PBMC) migration that is lost when NRVms are pre-treated with HuR inhibitor (J). All experimental groups in panels D–H received conditioned media. * $p \leq .05$. ** $p \leq .01$. *** $p \leq .001$.

of cardiac macrophages, but they are also capable of inducing migration in naïve PBMCs. A full proteomic profiling and relevant functional contributions of specific HuR-dependent secreted factors from myocytes that mediate this response would be a very worthwhile future endeavor. Functionally, this HuR-dependent early inflammatory cytokine and chemokine gene expression in myocytes from the ischemic myocardium may then contribute to the systemic innate immune response leading to the recruitment of monocytes to the injured myocardium and induction of pro-inflammatory gene networks in the cardiac macrophage population.

Our previous work identified HuR-dependent regulation of TGF β expression in myocytes as a likely paracrine cell-to-cell crosstalk mechanism of cardiac fibroblast activation during chronic pressure overload-induced remodeling.⁷ Our results here show a similar reduction in fibrosis and periostin expression indicative of reduced myofibroblast activity with HuR inhibition following an acute ischemic injury. However, additional work is needed to fully elucidate how HuR activity in cardiomyocytes functionally impacts other cardiac cell types, including fibroblasts, during pathological cardiac remodeling in response to both acute and chronic stressors. We have also independently shown that HuR is highly expressed in fibroblasts and is a critical mediator of cardiac myofibroblast activation in response to TGF β ,⁴⁰ while other recent work has suggested HuR activity in macrophages to mediate fibrosis and inflammation in diabetic cardiomyopathy.³³ Similarly, while our subsequent in vitro work clearly demonstrates a myocyte-driven effect of HuR, we cannot rule out contributions from other cell types in the myocardium contributing changes in HuR activity or total expression post-I/R. Taken together, these results demonstrate the complex nature of HuR activity among cell types in the heart, in addition to its function in mediating cell-to-cell communication, and raise the limitation that some of our observed protection here may be due to HuR inhibition in cardiac fibroblasts or macrophages in addition to cardiomyocytes. Nonetheless, our experiments using conditioned media transfer from isolated cells demonstrate a HuR-dependent myocyte-to-macrophage communication as at least a partial contributing mechanism.

An additionally noted limitation is the well-noted sex difference between cardiac I/R injury in males and females, with females being less susceptible to I/R injury. Given that the purpose of our study was to focus on the post-ischemic remodeling response of the myocardium, the use of only male mice assured a uniform response to the initial injury, allowing us to more accurately identify differences in the remodeling response. While this would also be a relevant response to investigate in female mice, it would require a different I/R protocol to yield the same remodeling response in control mice, as female mice have been broadly noted to have smaller initial infarct sizes compared to males.

Together, these new results and the existing literature make a strong case for HuR as a central player in cardiac remodeling with diverse roles in multiple cell types. We previously showed no deleterious cardiac phenotype in myocyte-specific deletion or pharmacological inhibition of HuR for 7 weeks in sham-treated wild-type mice, which supports further exploration of HuR inhibition as a promising therapeutic approach to reduce pathological cardiac remodeling.⁷

AUTHOR CONTRIBUTIONS

Michael Tranter and Samuel Slone designed the study and wrote the manuscript; Samuel Slone, Sarah R. Anthony, Lisa C. Green, Sharon Parkins, Pooja Acharya, Daniel A. Kasprovic, Kelsi Reynolds, Michelle L. Nieman, A. Phillip Owens, and Perwez Alam performed experiments; Samuel Slone, Sarah R. Anthony, Lisa C. Green, Daniel A. Kasprovic, Kelsi Reynolds, Robert M. Jagers, Zihai Li, John N. Lorenz, Onur Kanisicak, A. Phillip Owens, and Michael Tranter analyzed data and interpreted results; Xiaoqing Wu, Sudeshna Roy, Jeffrey Aubé, and Liang Xu contributed new reagents.

ACKNOWLEDGMENTS

This work was supported by NIH grants R01-HL132111 and R01-HL166326 (MT and OK), R01-HL148598 (OK), R01-CA191785 (LX and JA), R01-CA243445 (LX), R33-CA252158 (LX), and American Heart Association Career Development Award CDA34110117 (OK). SS was supported by the American Heart Association Predoctoral

Fellowship (PRE35230020). SP and LCG were supported by an NIH Training grant T32HL125204 (PIs: Molkentin and Kranias) and American Heart Association Predoctoral Fellowship awards (1029875 and PRE35210795, respectively). SP was also supported by the NIH Predoctoral Fellowship award (F31-HL170636). PA was supported by the American Heart Association Postdoctoral Fellowship (20POST35200267) and American Heart Association Career Development Grant (23CDA1052132). Graphical abstract and Figure 5A were created with BioRender.

DISCLOSURES


The authors state that there is no conflict of interest in connection with this research.

DATA AVAILABILITY STATEMENT

Genomic mapping of sequence reads and differential expression analysis was done using the Qiagen CLC Genomics Workbench (version 21.0.3). All RNA-Seq raw data files and total gene count files have been deposited in the NCBI GenBank (GSE accession number: 235081).

ORCID

Samuel Slone  <https://orcid.org/0000-0002-5073-9722>

Sarah R. Anthony  <https://orcid.org/0000-0002-6230-8188>

Lisa C. Green  <https://orcid.org/0000-0002-1164-6611>

Sharon Parkins  <https://orcid.org/0000-0003-2279-1598>

Pooja Acharya  <https://orcid.org/0000-0002-1877-6013>

Daniel A. Kasprovic  <https://orcid.org/0009-0004-1350-3755>

Kelsi Reynolds  <https://orcid.org/0009-0001-8201-7644>

Robert M. Jagers  <https://orcid.org/0000-0001-9613-7359>

Michelle L. Nieman  <https://orcid.org/0000-0001-8504-6697>

Perwez Alam  <https://orcid.org/0000-0002-7229-8008>

Xiaoqing Wu  <https://orcid.org/0000-0003-2076-4107>

Sudeshna Roy  <https://orcid.org/0000-0003-0237-4156>

Jeffrey Aubé  <https://orcid.org/0000-0003-1049-5767>

Liang Xu  <https://orcid.org/0000-0001-9196-4232>

Zihai Li  <https://orcid.org/0000-0003-4603-927X>

John N. Lorenz  <https://orcid.org/0000-0003-2161-9833>

A. Phillip Owens  <https://orcid.org/0000-0002-0835-620X>

Onur Kanisicak  <https://orcid.org/0000-0002-8393-4874>

Michael Tranter  <https://orcid.org/0000-0002-0609-3717>

REFERENCES

- Bacmeister L, Schwarzl M, Warnke S, et al. Inflammation and fibrosis in murine models of heart failure. *Basic Res Cardiol*. 2019;114:19.
- Ong S, Hernández-Reséndiz S, Crespo-Avilan G, et al. Inflammation following acute myocardial infarction: multiple players, dynamic roles, and novel therapeutic opportunities. *Pharmacol Ther*. 2018;186:73-87.
- Prabhu SD, Frangogiannis NG. The biological basis for cardiac repair after myocardial infarction: from inflammation to fibrosis. *Circ Res*. 2016;119:91-112.
- Srikantan S, Gorospe M. HuR function in disease. *Front Biosci*. 2012;17:189-205.
- Krishnamurthy P, Rajasingh J, Lambers E, Qin G, Losordo DW, Kishore R. IL-10 inhibits inflammation and attenuates left ventricular remodeling after myocardial infarction via activation of STAT3 and suppression of HuR. *Circ Res*. 2009;104:e9-e18.
- Krishnamurthy P, Lambers E, Verma S, et al. Myocardial knock-down of mRNA-stabilizing protein HuR attenuates post-MI inflammatory response and left ventricular dysfunction in IL-10-null mice. *FASEB J*. 2010;24:2484-2494.
- Green LC, Anthony SR, Slone S, et al. Human antigen R as a therapeutic target in pathological cardiac hypertrophy. *JCI Insight*. 2019;4:e121541.
- Dong R, Chen P, Polireddy K, et al. An RNA-binding protein, Hu-antigen R, in pancreatic cancer epithelial to mesenchymal transition, metastasis, and cancer stem cells. *Mol Cancer Ther*. 2020;19:2267-2277.
- Smiley D, Smith MA, Carreira V, et al. Increased fibrosis and progression to heart failure in MRL mice following ischemia/reperfusion injury. *Cardiovasc Pathol*. 2014;23:327-334.
- Ren X, Wang Y, Jones WK. TNF-alpha is required for late ischemic preconditioning but not for remote preconditioning of trauma. *J Surg Res*. 2004;121:120-129.
- Wu X, Gardashova G, Lan L, et al. Targeting the interaction between RNA-binding protein HuR and FOXQ1 suppresses breast cancer invasion and metastasis. *Commun Biol*. 2020;3(1):193. doi:10.1038/s42003-020-0933-1
- Liu R, Correll RN, Davis J, et al. Cardiac-specific deletion of protein phosphatase 1β promotes increased myofilament protein phosphorylation and contractile alterations. *J Mol Cell Cardiol*. 2015;87:204-213.
- Guarnieri AR, Anthony SR, Gozdiff A, et al. Adipocyte-specific deletion of HuR induces spontaneous cardiac hypertrophy and fibrosis. *Am J Physiol Heart Circ Physiol*. 2021;321:H228-H241.
- Willhide ME, Tranter M, Ren X, et al. Identification of a NF-κB cardioprotective gene program: NF-κB regulation of Hsp70.1 contributes to cardioprotection after permanent coronary occlusion. *J Mol Cell Cardiol*. 2011;51:82-89.
- Tranter M, Liu Y, He S, et al. In vivo delivery of nucleic acids via glycopolymer vehicles affords therapeutic infarct size reduction in vivo. *Mol Ther*. 2012;20:601-608.
- Tranter M, Ren X, Forde T, et al. NF-kappaB driven cardioprotective gene programs; Hsp70.3 and cardioprotection after late ischemic preconditioning. *J Mol Cell Cardiol*. 2010;49:664-672.
- Ehler E, Moore-Morris T, Lange S. Isolation and culture of neonatal mouse cardiomyocytes. *J Vis Exp*. 2013;79:50154.
- Slone S, Anthony SR, Wu X, et al. Activation of HuR downstream of p38 MAPK promotes cardiomyocyte hypertrophy. *Cell Signal*. 2016;28:1735-1741.
- Weischenfeldt J, Porse B. Bone marrow-derived macrophages (BMM): isolation and applications. *CSH Protoc*. 2008;2008:pdb.prot5080.

20. Zhang X, Goncalves R, Mosser DM. The isolation and characterization of murine macrophages. *Curr Protoc Immunol*. 2008;Chapter 14:14.1.1-14.1.14.
21. Livak KJ, Schmittgen TD. Analysis of relative gene expression data using real-time quantitative PCR and the 2⁻(Delta Delta C(T)) method. *Methods*. 2001;25:402-408.
22. Brown M, McGuinness M, Wright T, et al. Cardiac-specific blockade of NF-kappaB in cardiac pathophysiology: differences between acute and chronic stimuli in vivo. *Am J Physiol Heart Circ Physiol*. 2005;289:466.
23. Jones SM, Mann A, Conrad K, et al. PAR2 (protease-activated receptor 2) deficiency attenuates atherosclerosis in mice. *Arterioscler Thromb Vasc Biol*. 2018;38:1271-1282.
24. Anthony SR, Guarnieri A, Ianzillotta I, et al. HuR expression in adipose tissue mediates energy expenditure and acute thermogenesis independent of UCP1 expression. *Adipocytes*. 2020;9:335-345.
25. Huang DW, Sherman BT, Lempicki RA. Systematic and integrative analysis of large gene lists using DAVID bioinformatics resources. *Nat Protoc*. 2009;4:44-57.
26. Huang DW, Sherman BT, Lempicki RA. Bioinformatics enrichment tools: paths toward the comprehensive functional analysis of large gene lists. *Nucleic Acids Res*. 2009;37:1-13.
27. Owens AP 3rd, Passam FH, Antoniak S, et al. Monocyte tissue factor-dependent activation of coagulation in hypercholesterolemic mice and monkeys is inhibited by simvastatin. *J Clin Invest*. 2012;122:558-568.
28. Allegri L, Baldan F, Roy S, et al. The HuR CMLD-2 inhibitor exhibits antitumor effects via MAD2 downregulation in thyroid cancer cells. *Sci Rep*. 2019;9:7374.
29. Raguraman R, Shanmugarama S, Mehta M, et al. Drug delivery approaches for HuR-targeted therapy for lung cancer. *Adv Drug Deliv Rev*. 2022;180:114068.
30. Wang J, Hjelmeland AB, Nabors LB, King PH. Anti-cancer effects of the HuR inhibitor, MS-444, in malignant glioma cells. *Cancer Biol Ther*. 2019;20:979-988.
31. Majumder M, Chakraborty P, Mohan S, Mehrotra S, Palanisamy V. HuR as a molecular target for cancer therapeutics and immune-related disorders. *Adv Drug Deliv Rev*. 2022;188:114442.
32. Wu X, Xu L. The RNA-binding protein HuR in human cancer: a friend or foe? *Adv Drug Deliv Rev*. 2022;184:114179.
33. Govindappa PK, Patil M, Garikipati VNS, et al. Targeting exosome-associated human antigen R attenuates fibrosis and inflammation in diabetic heart. *FASEB J*. 2019;119:776-2251.
34. Nabors LB, Gillespie GY, Harkins L, King PH. HuR, a RNA stability factor, is expressed in malignant brain tumors and binds to adenine- and uridine-rich elements within the 3' untranslated regions of cytokine and angiogenic factor mRNAs. *Cancer Res*. 2001;61:2154-2161.
35. Jeyabal P, Thandavarayan RA, Joladarashi D, et al. MicroRNA-9 inhibits hyperglycemia-induced pyroptosis in human ventricular cardiomyocytes by targeting ELAVL1. *Biochem Biophys Res Commun*. 2016;471:423-429.
36. Cok SJ, Acton SJ, Morrison AR. The proximal region of the 3'-untranslated region of Cyclooxygenase-2 is recognized by a Multimeric protein complex containing HuR, TIA-1, TIAR, and the heterogeneous nuclear ribonucleoprotein U. *J Biol Chem*. 2003;278:36157-36162.
37. Matsumiya T, Ota K, Imaizumi T, Yoshida H, Kimura H, Satoh K. Characterization of synergistic induction of CX3CL1/ Fractalkine by TNF- α and IFN- γ in vascular endothelial cells: an essential role for TNF- α in post-transcriptional regulation of CX3CL1. *J Immunol*. 2010;184:4205-4214.
38. Yiakouvaki A, Dimitriou M, Karakasiliotis I, Eftychi C, Theocharis S, Kontoyiannis DL. Myeloid cell expression of the RNA-binding protein HuR protects mice from pathologic inflammation and colorectal carcinogenesis. *J Clin Invest*. 2012;122:48-61.
39. Zhang J, Modi Y, Yarovinsky T, et al. Macrophage β 2 integrin-mediated, HuR-dependent stabilization of angiogenic factor-encoding mRNAs in inflammatory angiogenesis. *Am J Pathol*. 2012;180:1751-1760.
40. Green LC, Slone S, Anthony SR, et al. HuR-dependent expression of Wisp1 is necessary for TGFbeta-induced cardiac myofibroblast activity. *J Mol Cell Cardiol*. 2022;174:38-46.

SUPPORTING INFORMATION

Additional supporting information can be found online in the Supporting Information section at the end of this article.

How to cite this article: Slone S, Anthony SR, Green LC, et al. HuR inhibition reduces post-ischemic cardiac remodeling by dampening myocyte-dependent inflammatory gene expression and the innate immune response. *The FASEB Journal*. 2025;39:e70433. doi:[10.1096/fj.202400532RRR](https://doi.org/10.1096/fj.202400532RRR)